International Journal of Thermophysics, Vol. 18, No. 5, 1997

A General Equation of State for Dense Fluids

G. Parsafar,[1,2] N. Farzi,[3] and B. Najafi[1]

Received February 26, 1997

A general equation of state, originally proposed for compressed solids by Parsafar and Mason, has been successfully applied to dense fluids. The equation was tested with experimental data for 13 fluids, including polar, nonpolar, saturated and unsaturated hydrocarbons, strongly hydrogen bonded, and quantum fluids. This equation works well for densities larger than the Boyle density ρ_B [$1/\rho_B = T_B\, dB_2(T_B)/dT$, where $B_2(T_B)$ is the second virial coefficient at the Boyle temperature, at which $B_2 = 0$] and for a wide temperature range, specifically from the triple point to the highest temperature for which the experimental measurements have been reported. The equation is used to predict some important known regularities for dense fluids, like the common bulk modulus and the common compression points, and the Tait–Murnaghan equation. Regarding the common points, the equation of state predicts that such common points are only a low-temperature characteristic of dense fluids, as verified experimentally. It is also found that the temperature dependence of the parameters of the equation of state differs from those given for the compressed solids. Specifically they are given by $A_i(T) = a_i + b_i T + c_i T^2 - d_i T \ln(T)$.

KEY WORDS: compressed fluid; equation of state; regularities.

1. INTRODUCTION

The statistical mechanical EOS which was derived by Ihm–Song–Mason [1] is not applicable for very dense fluids [2]. Another equation of state which was derived by Parsafar and Mason [2, 3], called the LIR, works very well for all types of dense fluids, for densities greater than the Boyle density but for temperatures below twice the Boyle temperature [2]. The purpose of this paper is to derive an EOS for dense fluids over a very wide

[1] Department of Chemistry, Isfahan University of Technology, Isfahan, 84154, Iran.
[2] To whom correspondence should be addressed.
[3] University of Tarbiat Modarres, Tehran, Iran.

0195-928X/97/0900-1197$12.50/0

temperature range, from the triple point to the highest temperature for which experimental data exist.

A universal equation of state has recently been derived for compressed solids [4], based on thermodynamic arguments applied to virial expansion of the internal energy, $E(\rho, T)$, and pressure, $p(\rho, T)$, in terms of density (ρ) and temperature (T), of the form

$$p(v/v_0)^2 = A_0 + A_1(\rho/\rho_0) + A_2(\rho/\rho_0)^2 \tag{1}$$

where $v_0 = 1/\rho_0$ is some standard volume, which is often taken to be the (molar) volume at $p = 0$, but which can be arbitrary. A_0, A_1, and A_2 are temperature-dependent parameters that depend on the type of substance and are given as

$$A_i(T) = T\left[C_{i+2} - (i+1) \int ((e_{i+1}(T))/T^2)\, dT \right], \qquad i = 0, 1, 2 \tag{2}$$

where C_{i+2} is a constant of integration, and where $e_{i+1}(T)$ are parameters for the coefficient of the internal energy E, such that

$$E = e_0(T) + e_1(T)\,\rho + e_2(T)\,\rho^2 + e_3(T)\,\rho^3 \tag{3}$$

For temperatures higher than the Debye temperature, $A_i(T)$ are given as

$$A_i(T) = a_i + b_i T - c_i T \ln(T) \tag{4}$$

The essential point in deriving the equation of state, Eq. (1), is to fit only the featureless repulsive branch of the binding energy curve rather than the entire curve for solids in compression. Note that Eq. (1) is a three-parameter equation of state, whose parameters can be simply obtained by fitting $p(v/v_0)^2$, as a quadratic function in terms of ρ/ρ_0, to high-pressure p–v–T data.

Now we anticipate that the same argument is also applicable to dense fluids in the entire temperature range, since the structure of a dense fluid is primarily determined by the short-range repulsive forces. Thus, in a sense we picture the repulsive part of the effective pair interaction potential as determining the structure of the dense fluid and the attractive part as holding the molecules together at some specified density [5]. Therefore, for dense fluids, the repulsive branch of the effective pair interaction potential can be represented by a similar functional form in density as solids, i.e., Eq. (3). This expectation will be tested with experimental p–v–T data of dense fluids. Such an expectation is not far from reality, as the Tait equation originally proposed for liquids in 1888 [6] and modified by Murnaghan

has been extensively used for both solids and liquids [7, 8] and, also, for dense supercritical fluids [9]. Therefore, we may expect that Eq. (1), which was originally derived for solids, may be applied to dense fluids as well.

2. EXPERIMENTAL TESTS

First, we check the validity of our prediction about the quadratic fit of pv^2 respect to ρ, Eq. (1), at very high and low temperatures. Equation (1) can be written in a dimensionless form as

$$(p/p_c)(v/v_c)^2 = A_0 + A_1(\rho/\rho_c) + A_2(\rho/\rho_c)^2 \tag{5}$$

or

$$p_r v_r^2 = A_0 + A_1 \rho_r + A_2 \rho_r^2 \tag{6}$$

where v_c and p_c are the critical volume and pressure of dense fluid, respectively.

Due to the abundance of accurate experimental p–v–T data of argon [10], $p_r v_r^2$ of argon is fitted as a quadratic function of ρ_r and the resulting curve is compared with the experimental data for $p_r v_r^2$ for the 1200 and 100 K isotherms in Figs. 1 and 2, respectively. The same calculation has been carried out for different isotherms of argon, for which the results are presented in Table I. The coefficient of determination [11] and the percentage deviation

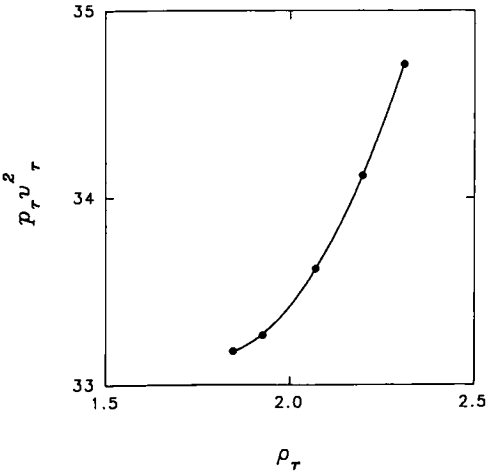

Fig. 1. Fitting the experimental data of argon with Eq. (6) at 1200 K.

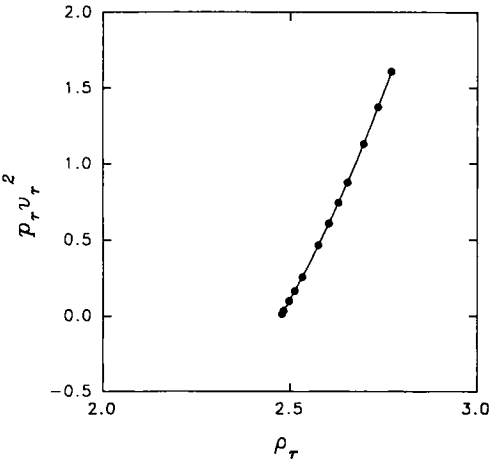

Fig. 2. Same as Fig. 1 for a 100 K isotherm.

Table I. Reduced Parameters (A_0, A_1, A_2) in Eq. (6), Coefficient of Determination (R^2), Pressure Range (Δp) of the Data, and Average Absolute Percentage Deviation of the Calculated Density at a Given Temperature for Argon[a]

T (K)	A_0	A_1	A_2	R^2	Δp (MPa)	$(100\,\lvert\Delta p\rvert/p)_{ave}$[b]
86	23.505 ± 1.614	−23.160 ± 1.213	5.397 ± 0.228	0.999998	0.1–8	0.062 (0.064)
100	16.729 ± 0.090	−17.684 ± 0.070	4.414 ± 0.013	1.000000	0.4–60	0.094 (0.11)
120	13.097 ± 0.226	−14.360 ± 0.182	3.838 ± 0.036	0.999983	1.5–150	0.055 (0.17)
140	10.831 ± 0.307	−12.096 ± 0.261	3.461 ± 0.055	0.999888	4–250	0.359 (2.52)
150	11.115 ± 0.456	−12.106 ± 0.379	3.499 ± 0.077	0.999855	10–300	0.323 (2.02)
200	13.657 ± 0.570	−12.979 ± 0.460	3.806 ± 0.090	0.999849	40–600	0.246 (1.45)
300	16.790 ± 0.494	−12.982 ± 0.388	3.969 ± 0.075	0.999900	100–900	0.117 (0.41)
400	19.955 ± 0.310	−12.970 ± 0.243	4.049 ± 0.047	0.999983	200–900	0.033 (0.11)
500	22.688 ± 0.179	−12.745 ± 0.146	4.061 ± 0.029	0.999994	250–900	0.033 (0.11)
600	25.994 ± 0.075	−13.024 ± 0.063	4.148 ± 0.013	0.999999	300–900	0.019 (0.03)
700	29.793 ± 0.067	−13.758 ± 0.059	4.313 ± 0.013	0.999999	300–900	0.006 (0.02)
800	33.782 ± 0.126	−14.705 ± 0.114	4.514 ± 0.025	0.999996	350–900	0.012 (0.02)
900	37.913 ± 0.172	−15.821 ± 0.159	4.746 ± 0.036	0.999994	400–900	0.020 (0.03)
1000	42.106 ± 0.259	−17.032 ± 0.243	4.995 ± 0.056	0.999990	450–900	0.010 (0.02)
1100	46.376 ± 0.320	−18.345 ± 0.305	5.264 ± 0.072	0.999989	500–900	0.005 (0.01)
1200	50.799 ± 0.425	−19.833 ± 0.411	5.572 ± 0.099	0.999986	550–900	0.004 (0.01)

[a] Data from Ref. 10.
[b] Maximum deviations are given in parentheses.

Table II. Same as Table I, for Different Fluids

Fluid	T (K)	A_0	A_1	A_2	R^2	Δp (MPa)	$(100\,\lvert\Delta\rho\rvert/\rho)_{ave}$
N_2[a]	1200	60.790 ± 0.657	-21.684 ± 0.609	5.986 ± 0.139	0.99999	450–1000	0.11 (0.13)
NH_3[b]	760	114.165 ± 3.705	-64.789 ± 3.49	20.279 ± 0.817	0.99995	250–500	0.022 (0.03)
C_6H_6[c]	410	23.228 ± 1.251	-23.683 ± 0.963	5.786 ± 0.185	0.99994	0.7–69	0.029 (0.06)
Iso-C_4H_{10}[d]	400	10.916 ± 0.260	-12.439 ± 0.255	3.692 ± 0.062	0.99995	35–55	0.072 (0.09)
CH_4[e]	400	15.129 ± 0.578	-11.001 ± 0.563	3.638 ± 0.137	0.99999	120–200	0.172 (0.19)
CH_3OH[d]	540	5.818 ± 0.116	-5.834 ± 0.109	1.703 ± 0.003	0.99999	25–70	0.026 (0.06)
H_2O[g]	773	5.690 ± 0.004	-4.751 ± 0.004	1.404 ± 0.001	1.00000	122–192	1.72 (1.88)
H_2[h]	100	16.760 ± 0.227	-9.155 ± 0.204	2.645 ± 0.045	0.99998	40–100	0.25 (0.28)
CO[i]	240	12.132 ± 0.050	-9.422 ± 0.051	3.189 ± 0.013	1.00000	60–100	0.332 (0.34)
C_2H_2[h]	423	13.276 ± 0.256	-12.410 ± 0.240	4.097 ± 0.559	0.99998	70–250	0.026 (0.06)
C_3H_8[h]	500	11.883 ± 0.269	-11.913 ± 0.269	4.013 ± 0.067	0.99999	50–100	0.005 (0.008)
$C_6H_5CH_3$[j]	800	10.483 ± 0.042	-10.145 ± 0.041	3.414 ± 0.010	1.00000	50–100	0.001 (0.002)

[a] Ref. 12.
[b] Ref. 13.
[c] Ref. 14.
[d] Ref. 15.
[e] Refs. 16 and 17.
[g] Ref. 18.
[h] Ref. 19.
[i] Ref. 20.
[j] Ref. 21.

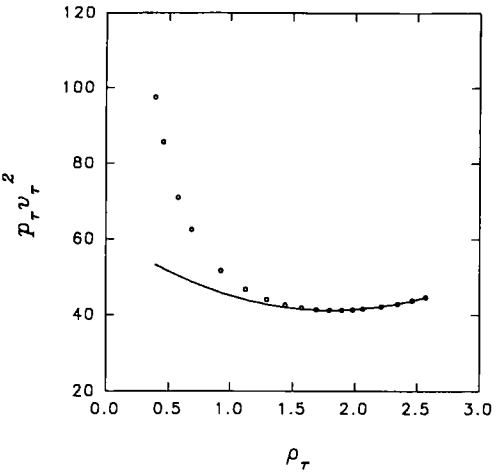

Fig. 3. Searching the lower density limit of Eq. (6) using the experimental data for nitrogen at 1200 K.

of the calculated density, compared to the experimental value are included. The maximum discrepancy is less than 2.6%, while the average deviation is less than 0.4%.

We have carried out similar comparisons with experimental data for different fluids, including quantum, aromatic, polar, nonpolar, and

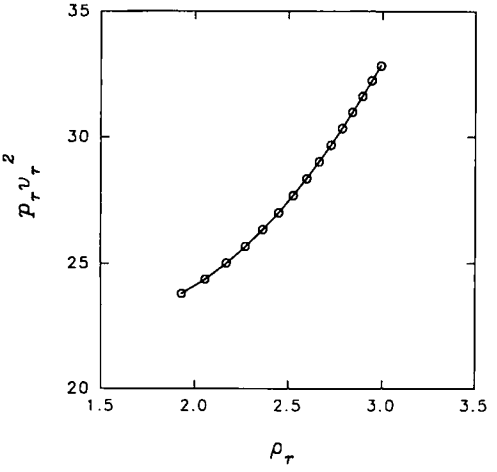

Fig. 4. Searching for the upper density limit of Eq. (6) using the experimental data for nitrogen at 400 K.

hydrogen-bonded compounds and the results are given in Table II [12–21]. We see that the quadratic fit is quite good. Therefore, we accept Eq. (1) as a general EOS for dense fluids in the entire temperature range. From now on, we call this equation of state DSEOS (abbreviated from "dense system equation of state"). The values of the parameters A_0, A_1, and A_2 at each temperature may be obtained from a quadratic fit of $p_r v_r^2$ to ρ_r.

To find the low- and high-density limits of the DSEOS, $p_r v_r^2$ has been quadratically fitted with respect to ρ_r in the entire density range for the 1200 K isotherm of N_2 [12] and is compared with the experimental $p_r v_r^2$ in Fig. 3. As shown in this figure, the quadratic fit is very good for densities above the Boyle density, $\rho_B \approx 1.8\rho_c$, which is about 20 mol · L^{-1} for N_2. While the low-density limit is the Boyle density, there is no indication for the upper-density limit as far as the experimental data exist [22] (see Fig. 4). The same conclusion is obtained for other isotherms of N_2 and also for other fluids.

3. TEMPERATURE DEPENDENCE OF PARAMETERS

Knowledge of the temperature dependence of the parameters of an EOS greatly increases the power of prediction from minimal input data.

The temperature dependencies of the parameters A_0, A_1, and A_2 of Eq. (6) are shown in Fig. 5 for N_2. The parameters have been fitted to Eq. (4) for solids. As shown in this figure, the data do not completely coincide with Eq. (4), and we anticipate that the temperature dependencies of the fluid parameters are different from those for the solid.

A derivation of Eq. (4) is based on the assumption that C_v is temperature independent, an assumption which is reasonable for solids at temperatures above the Debye temperature. Such an assumption should be investigated for dense fluids. Due to the unavailability of the variation of C_v with temperature at constant density, the summary of Stewart and Jacobsen [10] is used to obtain the variation of internal energy with density for different isotherms in a wide temperature range. As shown in Fig. 6, the internal energy may be fitted quite well with respect to ρ according to Eq. (3). The coefficients of the polynomials, $e_i(T)$, can be plotted versus temperature. The results are shown in Fig. 7. Unlike solids, we find that the e_i vary quadratically with T and not linearly. Of course, such a behavior is the reason that the parameters in Eq. (6) do not behave as those in Eq. (4). If we use a quadratic temperature dependence for each $e_i(T)$ in Eq. (2), we find

$$A_i(T) = a_i + b_i T + c_i T^2 - d_i T \ln(T), \qquad i = 0, 1, 2 \tag{7}$$

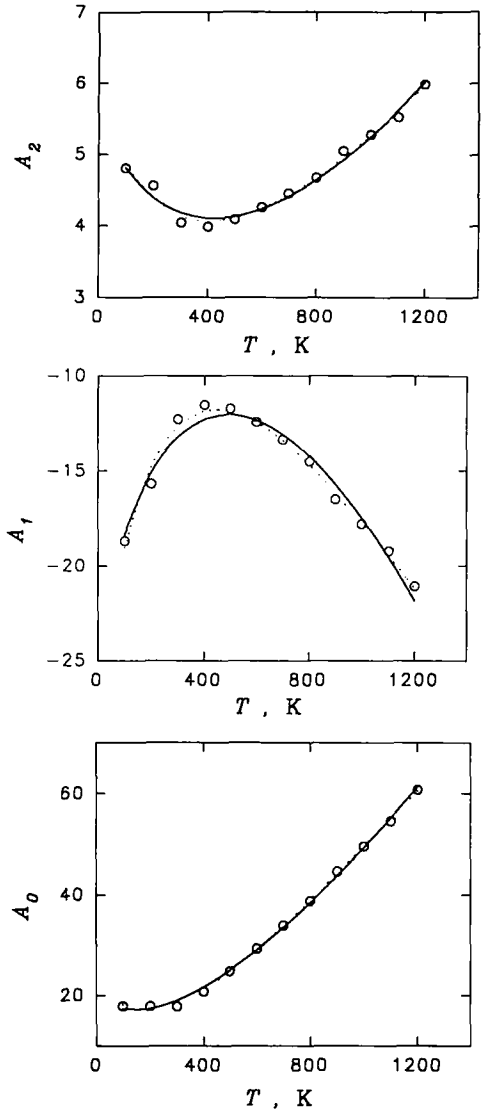

Fig. 5. The parameters of Eq. (6) obtained experimentally which are fitted with Eq. (4) (solid curve) and Eq. (7) (dotted curve).

where a_i, b_i, c_i, and d_i are constants (independent of both T and ρ). The values of the A_i in Eq. (7) are shown in Fig. 5. The values of a_i, b_i, c_i, and d_i may be obtained from a least-squares fit of Eq. (7) to the experimental results. The results obtained for Ar and N_2 are given in Table III.

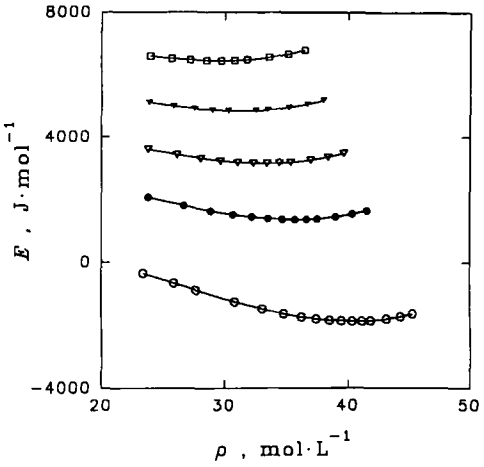

Fig. 6. The variation of the internal energy with respect to density for argon at 700 K (□), 600 K (▼), 500 K (▽), 400 K (●), and 240 K (○), fitted to Eq. (3).

4. REGULARITY PREDICTION

Any sensible equation of state is expected to verify the known regularities and also may be able to predict new regularities. In this section we discuss the regularities that can be deduced from DSEOS.

4.1. Common Compression Factor Point

Some equations of state predict a common intersection point for the compression factor, Z, versus ρ for different isotherms of a fluid. The three-shell modifications of the Lennard–Jones–Devonshire (LJD) [23], LIR [2, 3], and ISM [1] equations of state predict such a common intersection point, in agreement with experimental data [24].

The compressibility factor, Z, is given by DSEOS as

$$Z = (A_0\rho + A_1\rho^2 + A_2\rho^3)/RT \tag{8}$$

The numerical values of Z, given by Eq. (8), are plotted against ρ for different isothems of argon in the temperature range of 100–140 K in Fig. 8. The density of the common point given by the DSEOS, ρ_{OZ}, is 42.6 mol · L^{-1}, which is very close to the experimental value, 42.8 mol · L^{-1}.

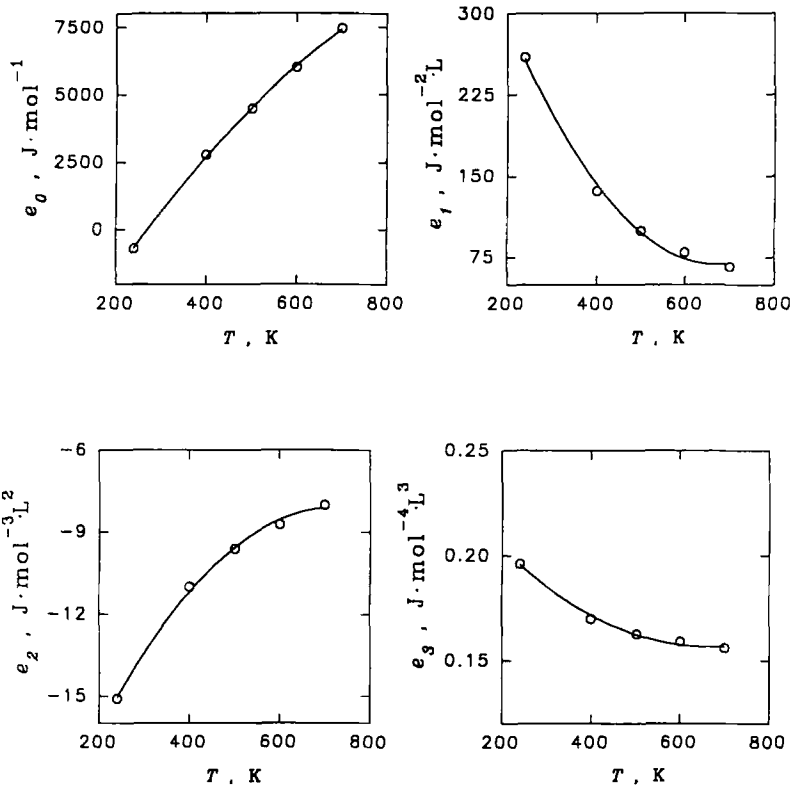

Fig. 7. The parameters of Eq. (3) fitted quadratically as a function of temperature for argon.

Table III. Constants of Eq. (7), $[A_i(T) = a_i + b_i T + c_i T^2 - d_i T \ln(T)]$, for Argon[a] and Nitrogen[b]

Fluid	Parameter of DSEOS	a_i	b_i (K^{-1})	$c_i \times 10^6$ (K^{-2})	$d_i \times 10^3$ (K^{-1})
Ar[a]	A_0	23.03 ± 2.461	-0.295 ± 0.071	-27.15 ± 10.51	-49.48 ± 11.44
	A_1	-24.88 ± 1.806	0.245 ± 0.052	16.85 ± 7.71	36.78 ± 8.393
	A_2	5.148 ± 0.332	-0.027 ± 0.0096	-1.433 ± 1.419	-4.098 ± 1.544
N_2[b]	A_0	26.690 ± 1.545	-0.344 ± 0.045	-25.440 ± 6.599	-56.820 ± 7.180
	A_1	-29.720 ± 1.397	0.332 ± 0.0403	20.910 ± 5.964	49.400 ± 6.490
	A_2	6.195 ± 0.318	-0.041 ± 0.0092	-1.943 ± 1.356	-6.096 ± 1.475

[a] Ref. 10.
[b] Ref. 12.

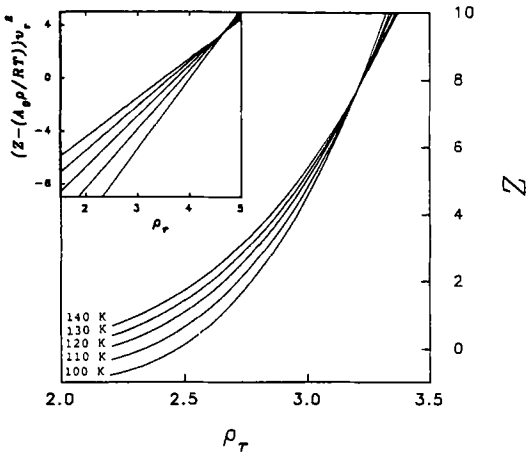

Fig. 8. Searching for the common compression point given by Eq. (8) and Eq. (10) (top left, using the experimental data on argon for given isotherms.

The DSEOS may be used to obtain the common compression point analytically. The density at this point can be obtained by setting $(\partial Z/\partial T)_{\rho_{OZ}}$ equal to zero, which gives

$$\sum_{i=0}^{2} (-a_i + c_i T^2 - d_i T)(\rho_{OZ})^{i+1} = 0 \tag{9}$$

At low temperatures, the $c_i T^2$ and $d_i T$ terms are negligible compared to a_i, and hence, ρ_{OZ} is a unique point (independent of temperature). But at high temperatures, where $c_i T^2$ and $d_i T$ are not negligible, the DSEOS predicts no common compression point. The above-mentioned equations of state (LJD, LIR, ISM) assert the existence of a common compression point but do not predict that such a regularity is a low-temperature behavior of fluid. The experimental value of Z against ρ is plotted for different isotherms of Ar in the temperature range of 800–1100 K in Fig. 9, which does not show any common intersection point. Therefore the DSEOS prediction seems to be in accordance with reality.

The reduced form of Eq. (8) may be rearranged into

$$(Z - A_0\rho/RT)\, v_r^2 = (A_1 + A_2\rho_r)/RT \tag{10}$$

which shows that a plot of $(Z - A_0\rho/RT)\, v_r^2$ versus ρ_r is linear, by which the intersection point can be determined more conveniently (see the top left-hand side in Fig. 8).

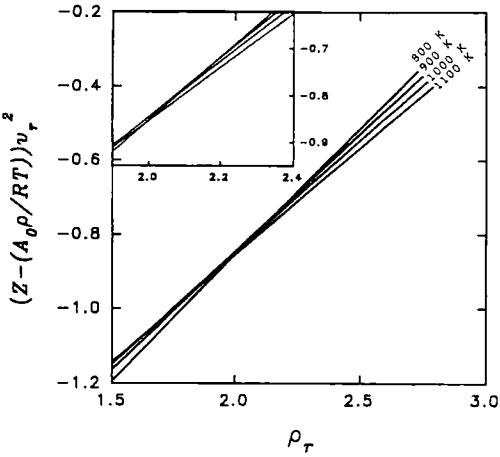

Fig. 9. Searching for the common compression point given by Eq. (10) for the high-temperature isotherms of argon (note that, unlike in Fig. 8, no common point exists).

In order to determine the density at the common compression point, ρ'_{OZ}, from Eq. (10), the following equation must be solved:

$$\{\partial[(Z-A_0\rho/RT)\,v_r^2]/\partial T\}_{(\rho'_{OZ}/\rho_c)}=0 \tag{11}$$

[The value of the density given by this equation, ρ'_{OZ}, differs from that given by Eq. (9), ρ_{OZ}. Using Eqs. (10) and (11) along with Eq. (7), we find

$$\frac{\rho'_{OZ}}{\rho_c}=\frac{a_1-c_1T^2+d_1T}{-a_2+c_2T^2-d_2T} \tag{12}$$

At low temperatures, where the c_iT^2 and d_iT terms are negligible, Eq. (12) reduces to

$$\frac{\rho'_{OZ}}{\rho_c}=\frac{a_1}{-a_2} \tag{13}$$

Using the values of a_1 and a_2 for Ar given in Table III, we find $(\rho'_{OZ}/\rho_c)=4.83$, and ρ'_{OZ} corresponds to $64.19\ \text{mol}\cdot\text{L}^{-1}$ (for Ar, $\rho_c=13.29\ \text{mol}\cdot\text{L}^{-1}$). The value of the calculated density at the intersection point is very close to the experimental value of $(\rho'_{OZ}/\rho_c)=4.56$ (see Fig. 8).

4.2. Common Bulk-Modulus Point

Recently, a new regularity in the behavior of the reduced bulk modulus, $B_r = (1/RT)(\partial p/\partial \rho)_T$, has been reported for liquids, where R is the gas constant. Huang and O'Connell [25] found that the isotherms of B_r versus molar volume intersect at a common point, called the common bulk-modulus point. They checked the existence of this point for more than 250 fluids. The value of B_r is independent of temperature at this point and ρ_{OB} is the density of the fluid at this point.

Using the DSEOS, we find

$$B_r = (2A_0\rho + 3A_1\rho^2 + 4A_2\rho^3)/RT \tag{14}$$

We have used Eq. (14) to calculate B_r of Ar for different isotherms. The results are shown in Fig. 10 for 100, 110, 120, 130, and 140 K isotherms, implying a common bulk-modulus point at 34.48 mol · L^{-1}.

The density at the common bulk-modulus point, ρ_{OB}, can be obtained by setting $(\partial B_r/\partial T)_{\rho_{OB}}$ equal to zero:

$$\sum_{i=0}^{2} (-a_i + c_i T^2 - d_i T)(\rho_{OB})^{i+1} = 0 \tag{15}$$

This equation shows that ρ_{OB} is temperature independent only at low temperatures, at which the temperature-dependent terms, namely, $c_i T^2$ and $d_i T$, are negligible compare to the temperature-independent terms, a_i.

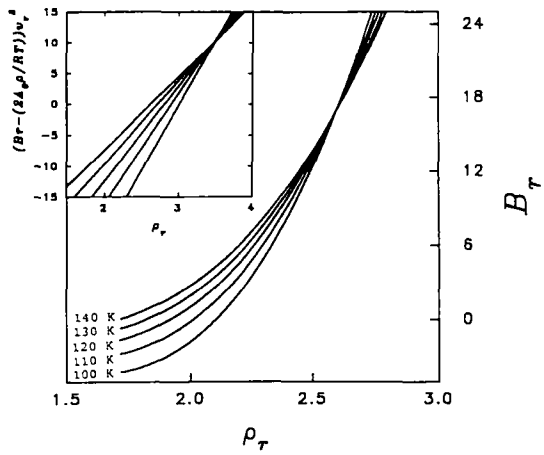

Fig. 10. Searching for the common bulk modulus point given by Eq. (14) and Eq. (16) (top left), using the experimental data on argon at given temperatures.

Equation (14) can be rearranged into

$$(B_r - 2A_0\rho/RT)\, v_r^2 = (3A_1 + 4A_2\rho_r)/RT \tag{16}$$

which shows that $(B_r - 2A_0\rho/RT)\, v_r^2$ versus ρ_r is linear for all isotherms of a dense fluid. Such a linear behavior is plotted in the top left-hand side in Fig. 10, for different isotherms of Ar from 100 to 140 K. Clearly, a common intersection point at $(\rho'_{OB}/\rho_c) = 3.45$ (corresponds to $\rho'_{OB} = 45.85$ mol · L^{-1}) exists.

A theoretical basis for the existence of such a point was recently developed by Boushehri et al. using the Ihm–Song–Mason EOS [26]. They found that

$$\rho_{OB} = \frac{1}{\lambda b_0} \tag{17}$$

where λ is the characteristic constant of the substance and b_0 is the molecular covolume at zero temperature. In another work, Najafi et al. [24] used the LIR EOS to find

$$\rho_{OB}^2 = 0.6\frac{A_1}{B_1} \tag{18}$$

Since A_1 and B_1 are temperature independent, the LIR predicts the existence of a common bulk-modulus point for each dense liquid analytically. In the following paragraph, we show that this result is valid only at low temperatures.

Using the DSEOS, at ρ'_{OB}, we must have

$$\{\partial[(B_r - 2A_0\rho/RT)\, v_r^2]/\partial T\}_{\rho'_{OB}/\rho_c} = 0 \tag{19}$$

or

$$\frac{\rho'_{OB}}{\rho_c} = \frac{3(a_1 - c_1 T^2 + d_1 T)}{4(-a_2 + c_2 T^2 - d_2 T)} \tag{20}$$

Equation (20) shows that ρ'_{OB} depends on T, except at low temperatures, where all temperature-dependent terms are negligible compared to a_1 and a_2 (see Table III). Therefore, at low temperatures Eq. (20) reduces to

$$\frac{\rho'_{OB}}{\rho_c} = \frac{-3a_1}{4a_2} \tag{21}$$

With the data in Table III for argon, Eq. (21) gives $\rho'_{OB} = 48.17\ \text{mol} \cdot \text{L}^{-1}$, which is very close to the experimental value $\rho'_{OB} = 45.85\ \text{mol} \cdot \text{L}^{-1}$ ($\rho_c = 13.29\ \text{mol} \cdot \text{L}^{-1}$ for Ar).

It is interesting to compare the ratio of ρ'_{OB}/ρ'_{OZ} given by different equations of state. From Eqs. (12) and (20), the DSEOS gives the following result:

$$\frac{\rho'_{OB}}{\rho'_{OZ}} = \frac{3}{4} \tag{22}$$

In the temperature range from 100 to 140 K we have for argon $(\rho'_{OZ}/\rho_c) = 4.56$ and $\rho'_{OB}/\rho_c = 3.45$, which gives $(\rho'_{OB}/\rho'_{OZ}) = 0.76$. Najafi et al. [24] used the LIR to obtain

$$\frac{\rho'_{OB}}{\rho'_{OZ}} = (0.6)^{0.5} \approx 0.77 \tag{23}$$

which is very close to the ratio given by the DSEOS.

4.3. Linearity of the Bulk Modulus Versus Pressure (Tait–Murnaghan Equation)

The origin of this regularity actually goes back to the empirical work of Tait on liquids in 1888 [6], in which the bulk modulus (reciprocal compressibility) of a liquid (or solid) is linear in pressure for each isotherm. Such a linearity is known as the Tait–Murnaghan equation [8],

$$B = B_0 + B'_0 p \tag{24}$$

where B_0 and B'_0 are temperature-dependent parameters. A theoretical basis for this equation has been given by Song et al. [27], using an equation of state based on statistical-mechanical perturbation theory.

The reduced bulk modulus, B_r, is plotted as a function of p in the 200–1200 K temperature range for argon in Fig. 11, in accordance with Eq. (14). As shown, at high temperatures and pressures a linear behavior is obtained in a very wide pressure range, which is in accordance with the results obtained by Alavi et al. [9].

Using a little algebra calculation, we find the following result from the DSEOS:

$$B_r = \frac{-A_0\rho + A_2\rho^3}{RT} + \frac{3}{\rho RT} p \tag{25}$$

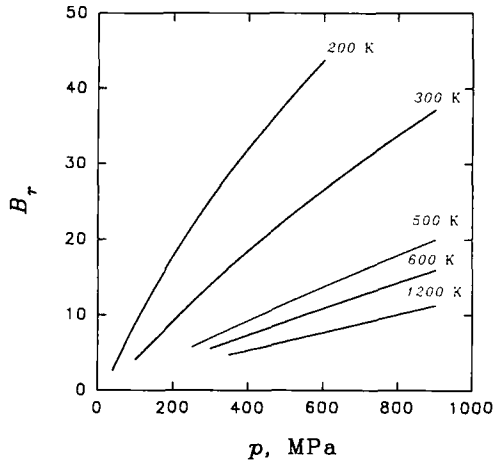

Fig. 11. The reduced bulk modulus in terms of pressure, using Eq. (25) for given isotherms of argon.

which is expected to be linear with respect to p for each isotherm of a dense fluid. It must be noted that although the density of a fluid depends on the pressure for each isotherm, this dependency is very weak for dense fluids. The variation of the slope of Eq. (25) with respect to p is given by

$$-\left[\frac{\partial(3/\rho RT)}{\partial p}\right]_T = \frac{3}{\rho RT}\kappa_T \tag{26}$$

where κ_T is the isothermal compressibility of the fluid. At high temperatures, the variation of the slope of Eq. (25) with pressure is small enough to be taken to be zero, a result which it not true at low temperatures. This prediction is consistent with the experimental data of Robertson and Babb [22]. The intercept of B_r versus p goes to zero at high temperatures, a result which is in agreement with Eq. (25).

5. COMPARISON OF LIR AND DSEOS

One of the recent equations of state derived for dense fluids is LIR, which simply predicts that $(Z-1)\,v_r^2$ varies linearly with respect to ρ_r^2, for each isotherm, as

$$(Z-1)\,v_r^2 = A + B\rho_r^2 \tag{27}$$

where A and B are temperature-dependent parameters of the fluid,

$$A = A_2 - \frac{A_1}{RT} \tag{28}$$

and

$$B = \frac{B_1}{RT} \tag{29}$$

where A_2, A_1, and B_1 are constants depending on the type of fluid.

Although it appears that LIR has a simpler form mathematically than the DSEOS, the LIR works only at temperatures below twice the Boyle temperature. However, the DSEOS does not have such a limitation. As shown in Fig. 12, $(Z-1)\,v_r^2$ as a function of ρ_r^2 has a large deviation from linearity for the 1200 K isotherm of argon. The coefficient of determination of LIR is given in Table IV, which may be compared with that of DSEOS given in Table I, to conclude that the former EOS is valid only for low temperatures ($T < 2T_B$), while the latter is valid for the entire temperature range, as far as the experimental data exist. This is the advantage of the DSEOS over the LIR.

The ability of the LIR and the DSEOS to predict the experimentally known regularities is comparable. However, the DSEOS has another advantage over the LIR to predict that the common bulk modulus and the

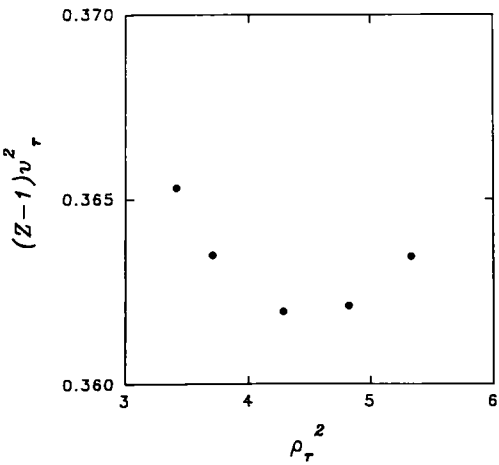

Fig. 12. The failure of LIR at high temperatures, using experimental data on argon at 1200 K.

Table IV. Reduced Parameters of LIR (A, B), the Coefficient of Determination (R^2), and the Pressure Range (Δp) for Argon[a] for Different Isotherms

T (K)	$A \times 10^3$	$B \times 10^4$	R^2	Δp (MPa)
86	-1679.4 ± 1.459	2197.3 ± 2.1	0.99999	0.1–8
100	-1302.4 ± 3.5	1858.8 ± 5.4	0.99992	0.4–60
120	-932.5 ± 4.1	1519.8 ± 6.9	0.99982	1.5–150
140	-696.8 ± 3.08	1309.0 ± 5.3	0.99987	4–250
150	-614.2 ± 3.6	1240.2 ± 5.8	0.99987	10–300
200	-307.3 ± 3.3	947.6 ± 4.3	0.99986	40–600
300	-9.6 ± 2.9	622.9 ± 3.8	0.99978	100–900
400	129.1 ± 2.3	444.1 ± 3.3	0.99973	200–900
500	207.4 ± 2.4	327.6 ± 3.7	0.99941	250–900
600	256.2 ± 2.6	245.0 ± 4.4	0.99868	300–900
700	293.8 ± 3.3	174.6 ± 6.1	0.99508	300–900
800	317.3 ± 3.4	124.3 ± 6.7	0.98984	350–900
900	334.7 ± 3.4	83.0 ± 7.2	0.97836	400–900
1000	348.0 ± 3.4	48.0 ± 7.4	0.94531	450–900
1100	358.7 ± 3.4	17.6 ± 7.6	0.75432	500–900
1200	367.3 ± 3.6	-9.4 ± 8.2	0.55045	550–900

[a] Ref. 10.

common compression points occur both only at low temperatures, as explained before. This low-temperature phenomenon has been reported experimentally by Boushehri et al. [26] for the common bulk-modulus point and, recently, for the isobaric expansivity by Deiters and Randzio [28]. As we showed, the DSEOS verifies that the existence of these common points is only a low-temperature characteristic of fluids.

The ratio of the density at two common points, ρ'_{OB}/ρ'_{OZ} is equal to 0.75 according to the DSEOS. It is interesting to note that this ratio is equal to $(0.6)^{0.5} = 0.77$ given by the LIR [24], so the two are very close to each other.

The behavior of B_r with respect to p has been studied with both the LIR and the DSEOS for both subcritical and supercritical fluids in a wide pressure range. It is interesting to note that the LIR gives the following relation for B_r with pressure:

$$B_r = 2(B\rho^4 - 1) + \left(\frac{3}{\rho RT}\right) p \tag{30}$$

whose slope is exactly the same as the slope given by the DSEOS [Eq. (25)].

6. CONCLUSION

An equation of state which was originally derived for solids was successfully applied for dense fluids by some modifications of its temperature-dependent parameters. Since the structure of a dense fluid is determined primarily by the short-range repulsive forces, like solids, its repulsive branch of the effective pair interaction potential can be represented by the same functional form in density as solids. The only major difference between the EOS of solids and that of dense fluids is the temperature dependencies of their parameters. The constancy of C_v with respect to T that applied for solids is not generally valid for dense fluids in a wide temperature range. Experimentally, we have noted that the C_v of a dense fluid varies with T linearly.

The DSEOS predicts that the common bulk modulus and common compression points exist only at low temperatures, a fact which is known experimentally [26, 28]. The ratio of the densities at these points (ρ'_{OB}/ρ'_{OZ}) implied by the DSEOS is 0.75, which is very close to the value 0.77 given by the LIR.

Finally, we obtained a very accurate equation of state for dense fluids, valid for all type of fluids, including polar, nonpolar, saturated, and unsaturated hydrocarbons and strongly hydrogen bonded, and quantum fluids (see Table II). It is valid for densities greater than the Boyle density at temperature from the triple point to the highest temperature for which the experimental data are available.

ACKNOWLEDGMENT

We wish to acknowledge the Isfahan University of Technology Research Council for the financial support.

REFERENCES

1. G. Ihm, Y. Song, and E. A. Mason, *J. Chem. Phys.* **94**:3839 (1991); *Fluid Phase Equil.* **75**:117 (1992).
2. G. A. Parsafar and E. A. Mason, *J. Phys. Chem.* **97**:9048 (1993).
3. G. A. Parsafar, *J. Sci. Islamic Repub. Iran* **2**:111 (1991).
4. G. A. Parsafar and E. A. Mason, *Phys. Rev. B* **49**:3049 (1994).
5. D. A. McQuarri, *Statistical Mechanics* (Harper & Row, New York, 1976).
6. J. H. Dymond and R. Malhotra, *Int. J. Thermophys.* **9**:941 (1988).
7. F. Birch, *J. Geophys. Res.* **83**:1257 (1978).
8. J. R. Macdonald, *Rev. Mod. Phys.* **40**:316 (1969).
9. S. Alavi, G. A. Parsafar, and B. Najafi, *Int. J. Thermophys.* **16**:1421 (1995).

10. R. B. Stewart and R. T. Jacobsen, *J. Phys. Chem. Ref. Data* **18**:639 (1989).
11. J. R. Taylor, *An Introduction to Error Analysis* (University Science Books, Mill Valley, CA, 1982), p. 180.
12. R. T. Jacobsen, R. B. Stewart, and M. Jahangiri, *J. Phys. Chem. Ref. Data* **15**:735 (1986).
13. L. Haar and J. S. Gallagher, *J. Phys. Chem. Ref. Data* **7**:635 (1978).
14. R. D. Goodwin, *J. Phys. Chem. Ref. Data* **17**:1541 (1988).
15. R. D. Goodwin, *J. Phys. Chem. Ref. Data* **16**:799 (1987).
16. B. A. Younglove and J. F. Ely, *J. Phys. Chem. Ref. Data* **16**:577 (1987).
17. U. Setzmann and W. Wagner, *J. Phys. Chem. Ref. Data* **20**:1061 (1991).
18. I. Tanishito, K. Watanabe, J. Kijima, H. Ishii, K. Oguchi, and M. Uematus, *J. Chem. Thermodyn.* **8**:1 (1976).
19. N. B. Vargaftik, *Hand Book of Physical Properties of Liquids and Gases*, 2nd ed., English translation (Hemisphere, New York, 1983).
20. R. D. Goodwin, *J. Phys. Chem. Ref. Data* **14**:849 (1985).
21. R. D. Goodwin, *J. Phys. Chem. Ref. Data* **18**:1565 (1989).
22. S. L. Robertson and S. B. Babb, Jr., *J. Chem. Phys.* **50**:4560 (1969).
23. J. O. Hirschfelder, C. F. Curtiss, and R. B. Bird, *Molecular Theory of Gases and Liquids*, 2nd printing (Wiley, New York, 1964), pp. 296–298.
24. B. Najafi, G. A. Parsafar, and S. Alavi, *J. Phys. Chem.* **99**:9248 (1995).
25. Y.-H. Huang and J. P O'Connell, *Fluid Phase Equil.* **37**:75 (1987).
26. A. Boushehri, F.-M. Tao, and E. A. Mason, *J. Phys. Chem.* **97**:2711 (1993).
27. Y. Song, B. Caswell, and E. A. Mason, *Int. J. Thermophys.* **12**:855 (1991).
28. U. K. Deiters and S. L. Randzio, *Fluid Phase Equil.* **103**:199 (1995).